J. Membrane Biol. 92, 171–182 (1986)

The Journal of
Membrane Biology
© Springer-Verlag New York Inc. 1986

Potential-Sensitive Response Mechanism of DiS-C_3-(5) in Biological Membranes

G. Cabrini and A.S. Verkman
Department of Medicine and Division of Nephrology, Cardiovascular Research Institute, University of California, San Francisco, California 94143

Summary. The potential-sensitive response mechanism of 3,3′-dipropylthiodicarbocyanine iodide (diS-C_3-(5)) was examined based on our previous model of diS-C_3-(5) interaction with brush border membrane vesicles (BBMV) in the absence of a membrane potential. The model contained binding (6 msec), reorientation (30 msec), dimerization (<10 nsec), and translocation (1 sec) reaction steps (Cabrini & Verkman, 1986. *J. Membrane Biol.* **90**:163–175). Transmembrane potentials (ψ) were induced in BBMV by K^+ gradients and valinomycin. Steady-state diS-C_3-(5) fluorescence (excitation 622 nm, emission 670 nm) increased linearly with ψ. The reorientation and translocation reaction steps were resolved by the stopped-flow technique as a biexponential decrease in fluorescence following mixture of diS-C_3-(5) with BBMV at varying ψ. The fractional amplitude of the faster exponential increased from 0.36 to 0.73 with increasing ψ (−17 to 87 mV); the time constant for the faster exponential (30–35 msec) was independent of ψ. There were single exponential kinetics (0.5–1.5 sec) for diS-C_3-(5) fluorescence response to a rapid (<2 msec) change in ψ in the absence of a diS-C_3-(5) concentration gradient. These results, and similar findings in placental brush border vesicles, red cell vesicles, and phosphatidylcholine vesicles, support a translocation mechanism for diS-C_3-(5) response, where induced membrane potentials drive diS-C_3-(5) redistribution between sites at the inner and outer membrane leaflets, with secondary effects on diS-C_3-(5) dimerization and solution/membrane partitioning. Fluorescence lifetime and dynamic depolarization measurements showed no significant change in diS-C_3-(5) rotational characteristics or in the polarity of the diS-C_3-(5) environment with changes in ψ. Based on the experimental results, a mathematical model is developed to explain the quantitative changes in diS-C_3-(5) fluorescence which accompany changes in ψ at arbitrary dye/lipid ratios.

Key Words cyanines · membrane potential · fluorescence lifetimes · brush border membrane · phosphatidylcholine vesicle

Introduction

The carbocyanine dye 3,3′-dipropylthiodicarbocyanine iodide (diS-C_3-(5)) has been used extensively to study membrane potentials in cell and vesicle suspensions (Waggoner, 1976; Kinnally, Tedeschi & Maloff, 1978; Wright, 1984). The fluorescence of diS-C_3-(5) typically changes by 0.2–0.5% per mV change in membrane potential with a response time of under 2 sec (Wright, Krasne, Kippen & Wright, 1981). The potential sensitive response mechanism of diS-C_3-(5) in biomembrane systems has been studied in several laboratories (Sims, Waggoner, Wang & Hoffman, 1974; Waggoner, Wang & Tolles, 1977; Tsien & Hladky, 1978; Ivkova, Pechatnikov & Ivkov, 1984). Effects of membrane potential on diS-C_3-(5) solution/membrane partitioning, intramembrane aggregation, and transmembrane redistribution have been proposed.

We have previously characterized the interaction mechanism for diS-C_3-(5) binding to renal brush border membrane vesicles (BBMV) in the absence of induced transmembrane potentials using stopped-flow and phase-modulation fluorescence methods (Cabrini & Verkman, 1986*a*) (Fig. 1). There is rapid binding of diS-C_3-(5) to the outer membrane surface (6 msec) followed by diS-C_3-(5) monomer reorientation (30 msec), very rapid dimerization (<10 nsec) and slow translocation (1 sec) to symmetric binding sites at the inner membrane leaflet. Fluorescence quenching studies of *n*-(9-anthroyloxy) fatty acids by diS-C_3-(5) showed that the diS-C_3-(5) monomer is oriented parallel and that the dimer is oriented perpendicular to the phospholipid chains (Cabrini & Verkman, 1986*b*), similar to findings for the merocyanine 540 binding orientation in hemispherical lipid bilayers (Dragsten & Webb, 1978).

In principle, any one or combination of the four reaction processes shown in Fig. 1 could be responsible for the change in diS-C_3-(5) fluorescence with induced transmembrane potentials. We report here a series of steady-state, stopped-flow and phase-modulation fluorescence experiments designed to determine the potential sensitive response mechanism of diS-C_3-(5) in BBMV and other biomembrane systems. The data support a model in which

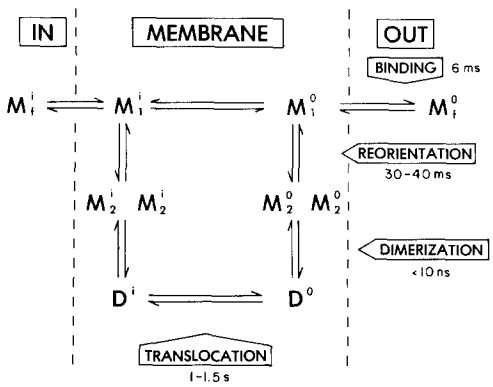

Fig. 1. Proposed mechanism for diS-C_3-(5) binding to brush border membranes. The major reaction processes and time constants are indicated. Symbols: M_f—aqueous monomer; M_1 and M_2—membrane bound monomer; D—membrane bound dimer. Superscripts i and o refer to diS-C_3(5) binding sites at the inner and outer membrane leaflets

diS-C_3-(5) redistribution between the outer and inner leaflets of the bilayer (translocation step) is primarily driven by induced transmembrane potentials, with secondary effects on diS-C_3-(5) dimerization and solution-membrane partitioning.

Materials and Methods

DiS-C_3-(5) was obtained from Molecular Probes Inc. (Seattle, WA) and was stored as a 2 mM stock solution in ethanol at 0°C in the dark. All other compounds were obtained from Sigma Chemical Co. (St. Louis, MO). Acrylic cuvettes (Starstedt, W. Germany) were used to minimize dye binding.

Membrane Preparations

BBMV were prepared from rabbit renal cortex by homogenization, Mg aggregation, and differential centrifugation as described previously (Booth & Kenny, 1974). Buffer consisted of 250 mM sucrose, 10 mM HEPES/Tris, pH 7.4, with variable KCl and choline Cl to keep ionic strength constant ([KCl] + [choline Cl] = 150 mM). Placental microvillous membrane vesicles (MVV) were prepared from fresh human placenta by isotonic stirring, Mg aggregation, and differential centrifugation (Booth, Olaniyan & Vanderpuye, 1980). Buffer consisted of 100 mM sucrose, 10 mM HEPES/Tris, pH 7.4, and 150 mM (KCl + choline Cl). Sealed red cell ghost membranes were prepared by the method of Steck and Kant (1974) in buffer consisting of 10 mM HEPES/Tris, pH 7.4, and 150 mM (KCl + choline Cl). Membrane potentials were induced by adding valinomycin (50 μg/mg membrane protein) from a 25 mg/ml stock solution in ethanol to vesicles having preformed KCl gradients. There was no effect of ethanol (<0.5% vol/vol) on diS-C_3-(5) fluorescence.

Unilamellar phosphatidylcholine (PC) vesicles were prepared by probe sonication of ~25 mM PC for 45 min at 4°C under N_2 (Huang & Thompson, 1974). Buffers consisted of 80 mM Tris/HCl, pH 7.4, and 150 mM (KCl + choline Cl). Membrane potentials were induced by adding valinomycin (30 μg/μmol PC).

Stopped-Flow Experiments

Stopped-flow measurements were performed on a Dionex 130 stopped-flow apparatus (Sunnyvale, CA) interfaced to a MINC/23 computer (Digital Equipment Corp., Maynard, MA). The instrument dead time was <2 msec and the maximum rate of data acquisition was 25 kHz. The excitation wavelength was 622 nm as set by a Zeiss double monochromator; emission light was filtered by Corion 650 or 695 cut-on filters.

Fluorescence Experiments

Steady-state fluorescence intensity and anisotropy measurements were performed on an SLM 8225 fluorimeter (Urbana, IL) using photon counting detection. Anisotropy (excitation 622 nm, emission 695 nm, 8 nm slits) was measured using Glan-Thompson polarizers in the T-format; less than 0.5% of detected light was due to scattering.

Fluorescence lifetime and dynamic depolarization measurements were performed on an SLM 4800 fluorimeter as described previously (Cabrini & Verkman, 1986*a*). Excitation light (622 nm) was selected with a monochromator and emission light was filtered by Schott 697 nm sharp cut-on filters. For lifetime studies, an isochronal standard was used (Barrow & Lentz, 1983) consisting of diS-C_3-(5) in ethylene glycol. The phase lifetimes of 3 μM diS-C_3-(5) in ethylene glycol were 2.08 nsec (30 MHz), 2.10 nsec (18 MHz) and 2.08 nsec (6 MHz) measured using a dilute glycogen reference solution. The mean lifetime, 2.09 nsec, did not vary with diS-C_3-(5) concentration. Sample and reference intensities were matched to within 5% in all measurements.

In some experiments the time course of phase lifetime or differential tangent (tan Δ) was measured before and during induction of a transmembrane potential with valinomycin addition. Phase angles were recorded after every 2.5 sec data accumulation period by an IBM-XT computer. Time courses were acceptable only if the phase angle of a diS-C_3-(5)/ethylene glycol standard changed by less than 0.1° (30 MHz) from the beginning to the end of the run. >75% of runs were acceptable after a 3-hr instrument warmup time.

Results

DiS-C_3-(5) Potential-Dependent Response Mechanism

The first series of experiments are designed to determine which of the reaction processes shown in Fig. 1 are sensitive to induced transmembrane potentials. The approach will be to resolve the relative binding of diS-C_3-(5) to sites on each half of the bilayer in the presence of induced transmembrane potentials. The response kinetics for a change in diS-C_3-(5) fluorescence driven by electrical potential will then be compared to the kinetics for the individual reaction processes in Fig. 1.

Transmembrane electrical potentials were created by K^+ gradients in the presence of valinomycin as described previously (Beck & Sacktor, 1978; Wright et al., 1981). Figure 2 shows the effect of

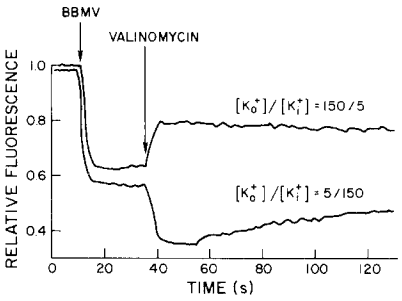

Fig. 2. DiS-C_3-(5) fluorescence response to an induced membrane potential. BBMV (30 μM membrane phospholipid) containing 5 or 150 mM KCl added to 3 μM diS-C_3-(5) in 150 or 5 mM KCl. Relative fluorescence (excitation 622 nm, emission 670 nm) was measured as a function of time. Membrane potentials were induced by addition of valinomycin

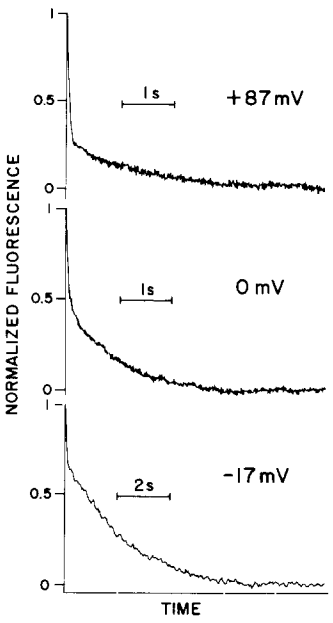

Fig. 3. Time course of diS-C_3-(5) binding to BBMV having different potentials. BBMV (60 μM membrane phospholipid) containing valinomycin mixed with an equal volume of 10 μM diS-C_3-(5) in a stopped-flow apparatus. Specified membrane potentials induced at the time of mixing by establishing KCl gradients ($[K^+]_{out}/[K^+]_{in}$ = 152/5, +87 mV; 150/150, 0 mV; 152/300, −87 mV). The time course of diS-C_3-(5) fluorescence (excitation 622 nm, emission >650 nm) was biexponential; fitted time constants and amplitudes are given in Table 1

membrane potential on steady-state diS-C_3-(5) fluorescence. Addition of BBMV results in a decrease in fluorescence at the emission wavelength of the aqueous diS-C_3-(5) monomer (670 nm) due to membrane partitioning. K^+ was replaced with an equivalent amount of choline$^+$ to avoid osmotic gradients. In the absence of valinomycin, ψ is set from inside and outside K^+ and Cl^- concentrations according to the Goldman equation,

$$\psi = 59 \text{ mV} \log \frac{[K^+]_{out} + (P_{Cl}/P_K)[Cl^-]_{in}}{[K^+]_{in} + (P_{Cl}/P_K)[Cl^-]_{out}} \quad (1)$$

where P_{Cl}/P_K is the ratio of electrogenic Cl^- to K^+ permeabilities in BBMV which has been estimated to be 0.8 ± 0.1 using the bi-ionic potential method (Gunther, Shell & Wright, 1984). For $[K^+]_{out}/[K^+]_{in}$ = 150/5 and 5/150 mM (Fig. 2) ψ is +19.7 and −19.7 mV, respectively, before valinomycin addition and +87 and −87 mV after valinomycin addition when $P_K \gg P_{Cl}$. Addition of valinomycin causes a rapid change in diS-C_3-(5) fluorescence (<3 sec, fluorimeter mixing time) followed by a slower time course due in part to dissipation of the K^+ gradient. Addition of valinomycin in the absence of a K^+ gradient does not alter steady-state fluorescence intensity (*not shown*). We have confirmed that steady-state fluorescence intensity varies linearly with ψ in the range −87 to +87 mV with slopes 0.30%/mV (depolarizing) and −0.45%/mV (hyperpolarizing) similar to data presented by Beck and Sacktor (1978) and Wright et al. (1981).

When low concentrations of BBMV are mixed with diS-C_3-(5) in a stopped-flow apparatus in the absence of a membrane potential (Fig. 3, 0 mV), there is a biexponential decrease in fluorescence due to diS-C_3-(5) reorientation/dimerization (30–40 msec, *see* Fig. 1) followed by translocation of diS-C_3-(5) dimer from binding sites at the outer to inner membrane leaflets (Cabrini & Verkman, 1986*a*). For the low BBMV concentrations used in experiments in Fig. 3, the amplitudes of the fast and slow exponential processes, representing decreased aqueous diS-C_3-(5) due to membrane binding, are proportional to the number of diS-C_3-(5) molecules bound at the outer and inner leaflets of the membrane, respectively.

Similar stopped-flow experiments were performed in the presence of induced membrane potentials by mixing solutions containing BBMV + valinomycin with diS-C_3-(5); the solutions contained different K^+ concentrations to establish a membrane potential immediately after mixing (Fig. 3 and Table 1). There was a biexponential time course of decreasing fluorescence in every experiment. The fractional signal amplitude of the fast component increased from 0.36 to 0.73 as interior membrane potential increased from −17 to +87 mV. These results indicate that a redistribution of diS-C_3-(5) molecules between sites at the inner and outer membrane leaflets occurs in response to a membrane potential. As predicted for an electrostatic interaction, an interior negative potential favors redistribution of positively charged diS-C_3-(5) from sites at the outer to inner membrane leaflets.

Table 1. Membrane potential effects on the binding kinetics of DiS-C_3-(5) to BBMV

$[K^+]_{out}/[K^+]_{in}$ (mM)	ψ (mV)	τ_{fast} (msec)	τ_{slow} (sec)	A_{fast}/A_{tot}	n
152/5	+87	36 ± 4	1.1 ± 0.1	0.74 ± 0.04	6
77/5	+70	42 ± 2	0.6 ± 0.1	0.69 ± 0.04	3
12/5	+23	45 ± 6	0.2 ± 0.2	0.69 ± 0.03	5
150/150	0	36 ± 2	1.0 ± 0.1	0.53 ± 0.03	8
152/300	−17	47 ± 6	1.9 ± 0.3	0.36 ± 0.06	5

BBMV (60 μM membrane phospholipid + valinomycin) containing specified $[K^+]_{in}$ was mixed in a stopped-flow apparatus with 10 μM diS-C_3-(5) to obtain the specified K^+ gradient. Fluorescence was measured at >650 nm. The time course of decreasing fluorescence (F) (*see* Fig. 3) was fitted to a biexponential, $F = A_{fast}\exp(-t/\tau_{fast}) + A_{slow}\exp(-t/\tau_{slow})$ with $A_{tot} = A_{fast} + A_{slow}$. Experiments were performed n times; errors are 1 SD.

In addition, the data in Table 1 show no systematic effect of membrane potential on the exponential time constant for the fast component of the curve. These results are consistent with the conclusion that there is no direct effect of membrane potential on the equilibrium constant for intramembrane diS-C_3-(5) dimerization (*see* below). Table 1 shows a complex effect of membrane potential and K^+ concentration on the exponential time constant for the slow component which cannot be interpreted on the basis of a single effect. The slow time constant is determined by the rate of translocation of a single diS-C_3-(5) unit and on the number of diS-C_3-(5) units which must be translocated to reach equilibrium. The rate for translocation of a single unit is determined by the detailed intramembrane potential profile (*see* Fig. 8), which depends upon the transmembrane potential. The number of units that must be translocated increases with interior negative membrane potentials as shown by the dependence of A_{fast}/A_{tot} on membrane potential discussed above. In addition, there may be direct effects of K^+ concentration on diS-C_3-(5) partitioning into the membrane interior, and thus on the intramembrane potential profile for diS-C_3-(5) translocation.

The results in Fig. 3 and Table 1 indicate that diS-C_3-(5) redistribution is associated with a change in membrane potential, but give no information about whether redistribution is driven by membrane potential. DiS-C_3-(5) redistribution could occur indirectly, due to an effect of membrane potential on other reaction processes. In order to examine which reaction process is driven directly by a change in transmembrane potential, the diS-C_3-(5) response time was measured. It was necessary to design an experiment in which membrane potential could be changed rapidly (<2 msec) without imposing a diS-C_3-(5) concentration gradient. Because of the finite

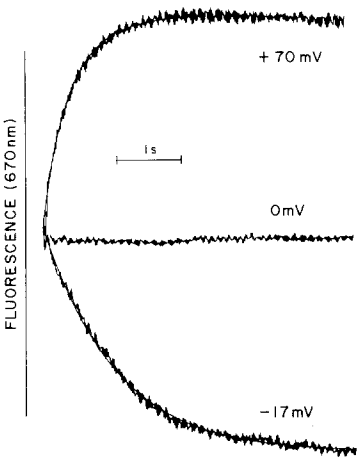

Fig. 4. Time course of diS-C_3-(5) response to induced transmembrane potentials. Membrane potentials were induced by KCl gradients in the absence of diS-C_3-(5) concentration gradients. *0 mV:* BBMV (30 μM membrane phospholipid, 5 mM KCl) containing 3 μM diS-C_3-(5) in the absence of valinomycin was mixed in a stopped-flow apparatus with an equal volume of 150 mM KCl containing ~0.5 μM diS-C_3-(5) to give no change in diS-C_3-(5) fluorescence with time. *+70 mV:* Same experiment repeated with valinomycin added to the BBMV. Single exponential fitted time constant was 0.5 sec. *−17 mV:* The same procedure used for the 0/+70 mV potentials was repeated using BBMV containing 150 mM KCl, 3 μM diS-C_3-(5) mixed with 5 mM KCl, ~0.5 μM diS-C_3-(5). DiS-C_3-(5) fluorescence remained constant in the absence of valinomycin and decreased exponentially (τ = 1.1 sec) when valinomycin was added

time required for valinomycin to insert into the membrane and exert its effect, an instantaneous membrane potential change could not be induced by addition of valinomycin to BBMV as in Fig. 2. The stopped-flow experiments in Fig. 3 are also inadequate because a diS-C_3-(5) concentration gradient is present.

The approach used to measure the diS-C_3-(5) response time is shown in Fig. 4. BBMV containing 3 μM diS-C_3-(5) and a specified K^+ concentration were mixed with an equal volume of a solution containing a different K^+ concentration and several diS-C_3-(5) concentrations. The diS-C_3-(5) concentration was determined in which there was no time dependence of the fluorescence response and thus no diS-C_3-(5) concentration gradient (0 mV, Fig. 4). The same experiment was repeated with valinomycin added to the BBMV prior to mixing; under these conditions any change in fluorescence is due exclusively to a change in membrane potential. The fluorescence response to +70 and −17 mV induced potentials follows a single exponential closely with time constants similar to those measured for the translocation reaction. In eight measurements (−17 to +87 mV) performed using 650 or 695 nm cut-on

Table 2. DiS-C_3-(5) response kinetics in biological membranes

	BBMV	RBC Ghosts	MVV	PC
Reaction time constants for membranes at 0 mV				
Binding (msec)	6 ± 1	19 ± 5	11 ± 1	3.4 ± 0.3
Reorientation (msec)	31 ± 1	35 ± 5	27 ± 1	120 ± 17
Translocation (sec)				
Dimer	0.9 ± 0.1	0.97 ± 0.06	0.53 ± 0.05	4.8 ± 0.4
Monomer	4.1 ± 0.1		30 ± 2	32 ± 1
Response times for membrane potential perturbations				
+70 mV (sec)	0.5 ± 0.2	0.5 ± 0.1	16 ± 2	
−17 mV (sec)	1.2 ± 0.1	0.8 ± 0.1	3.8 ± 0.4	4.9 ± 0.4

The time constants for the binding, reorientation and translocation processes were determined by the stopped-flow method using 3 μM diS-C_3-(5) as described previously (Cabrini & Verkman, 1986*a*). Membrane concentrations for the reorientation and dimer translocation studies were: BBMV (30 μM membrane phospholipid), RBC ghosts (300 μg protein/ml), MVV (400 μg protein/ml) and PC vesicles (20 μM lipid). For the binding and monomer translocation studies, membrane concentrations were 5–10 times higher. The response to an induced membrane potential was measured in the absence of a diS-C_3-(5) concentration gradient as in Figs. 4 and 5. Measurements were performed in quadruplicate; errors are 1 SD.

filters on the emission light there was no evidence for the presence of any reaction process faster than 0.4 sec. These findings indicate that it is the translocation reaction, and not the dimerization or initial binding reaction, that is driven by changes in transmembrane potential.

In order to determine whether this translocation mechanism applies to other biological and artificial membranes, the experiments shown in Fig. 4 were performed using sealed red cell ghost membranes, human placental microvillous membrane vesicles, and unilamellar phosphatidylcholine vesicles. The kinetics for individual reaction processes in membranes voltage clamped to 0 mV are given in Table 2. The time constants for the reorientation and dimer translocation processes were determined from a biexponential fit to the time course of decreasing fluorescence (>650 nm) for mixture of membranes at low concentrations with 3 μM diS-C_3-(5) (*see* Fig. 3, 0 mV). The time constants for the initial binding and monomer translocation processes were estimated from the time course of increasing fluorescence (>695 nm) for mixture of membranes at high concentrations with diS-C_3-(5) (Cabrini & Verkman, 1986*a*). The time constant for diS-C_3-(5) fluorescence response to a change in membrane potential was measured for each membrane (Fig. 5 and Table 2). For BBMV, RBC ghosts, and PC vesicles, the response time for a membrane potential change is very similar to the time constant for the dimer translocation reaction, and much greater than the time constants for the binding and reorientation reactions. The data are less clearcut for the MVV; the time constants for membrane potential change are very different for +70 and −17 mV potentials and

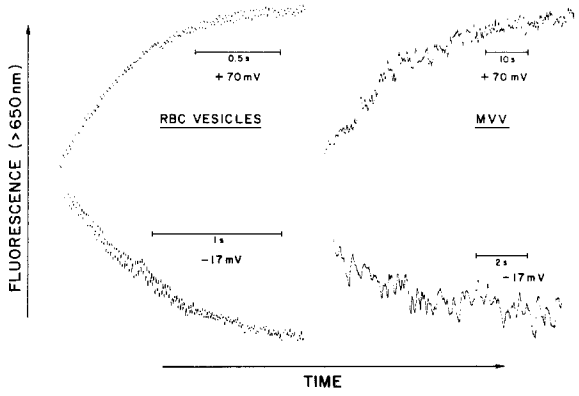

Fig. 5. DiS-C_3-(5) response time in red cell ghosts, MVV and PC vesicles. The experiment performed in Fig. 4 was repeated in three additional membrane preparations. The time course of diS-C_3-(5) to an induced membrane potential is shown. Concentrations and fitted time constants are given in Table 2

may represent a translocation mechanism with asymmetric binding of diS-C_3-(5) to each membrane leaflet. These results suggest that membrane potential-driven diS-C_3-(5) translocation is a general mechanism valid in both biological and artificial membrane systems.

diS-C_3-(5) Mobility and Membrane Environment

The next series of studies were designed to examine whether membrane potential modifies the binding location and the rotational characteristics of the membrane-bound diS-C_3-(5) monomer. We showed previously that the diS-C_3-(5) fluorescence lifetime

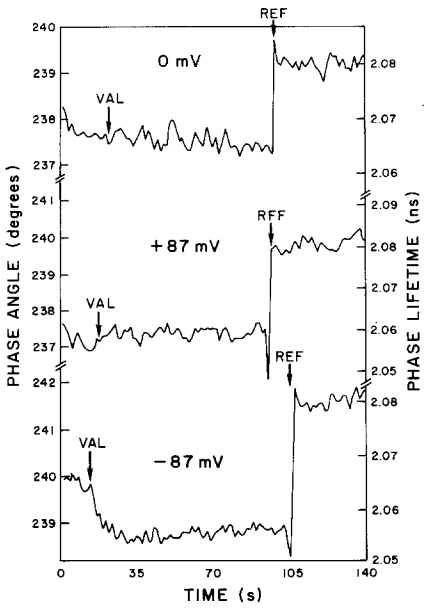

Fig. 6. DiS-C_3-(5) lifetime response to membrane potential. Membrane potentials were induced by valinomycin addition to BBMV (200 μM membrane phospholipid) + 3 μM diS-C_3-(5) as in Fig. 2. The time course of the phase angle at a 30-MHz modulation frequency was recorded. The reference solution consisted of diS-C_3-(5) in ethylene glycol as described in Materials and Methods. Measured lifetimes are given in Table 2

Table 3. Membrane potential effects on diS-C_3-(5) fluorescence properties

(mV)	VAL	τ (nsec)	r	tan Δ	R nsec^{-1}	r_∞
0	−	2.070	0.1095	0.0193	0.60	0.0747
		±0.001	±0.0003	±0.0007	±0.02	±0.0004
	+	2.067	0.1098	0.0185	0.63	0.0752
		±0.001	±0.0002	±0.0015	±0.05	±0.0009
+87	−	2.066	0.1122	0.0143	0.83	0.0864
		±0.003	±0.0004	±0.0013	±0.08	±0.0013
	+	2.064	0.1175	0.0175	0.63	0.0886
		±0.002	±0.0002	±0.0015	±0.05	±0.0012
−87	−	2.071	0.1118	0.0169	0.71	0.0757
		±0.002	±0.0004	±0.0005	±0.02	±0.0005
	+	2.062	0.1131	0.0175	0.64	0.0848
		±0.003	±0.0003	±0.0005	±0.02	±0.0005

Abbrev.: VAL, valinomycin; τ, fluorescence phase lifetime; r, steady-state anisotropy; tan Δ, differential tangent; R, rotational rate; r_∞, limiting anisotropy. Solutions consisted of BBMV (200 μM membrane phospholipid) and 3 μM diS-C_3-(5). All measurements were performed at an 18-MHz modulation frequency (*see* Materials and Methods). Membrane potentials were created as in Fig. 2; − and + refer to before and after valinomycin addition. '+' Measurements were performed within 30 sec after valinomycin addition. The diS-C_3-(5) lifetime was homogeneous under all conditions as determined by agreement among phase and modulation lifetimes at 18 and 30 MHz. Errors are 1 SD for quadruplicate determinations.

is a sensitive measure of solvent polarity and that dynamic depolarization methods could be used to define the diS-C_3-(5) rotational rate (R) and the degree to which rotation is hindered (r_∞, limiting anisotropy) assuming isotropic diS-C_3-(5) rotation in the membrane (Cabrini & Verkman, 1986*a*). Similar phase-modulation measurements are now performed in the presence of membrane potentials induced by K^+ gradients and valinomycin as in Fig. 2. In order to improve the accuracy of phase angle determinations for lifetime and tan Δ measurements, the effects of valinomycin on the time course of phase angle were measured as shown in Fig. 6. Differences in phase angle of 0.2 degrees corresponding to a phase lifetime of 2 psec could be resolved by this method.

Table 3 summarizes the effects of membrane potential on the measured fluorescence lifetime (τ), steady-state anisotropy (r), and differential tangent (tan Δ) for the membrane bound diS-C_3-(5) monomer, and on the calculated parameters R and r_∞. In the absence of a K^+ gradient (0 mV), addition of valinomycin does not significantly alter any of the measured or calculated quantities. Addition of valinomycin in the presence of K^+ gradients, resulting in +87 and −87 mV induced potentials, causes small increases in r and r_∞, and decreases in R significant to the $P < 0.05$ level (Student's t test, r_∞ at +87 mV not significant). These surprising results suggest that an induced membrane potential of any sign causes a small decrease in the rotational mobility of the diS-C_3-(5) monomer. Lelkes (1979) found that membrane potentials of any sign (0 to ±100 mV) caused an increase in the steady-state anisotropy of diphenylhexatriene in PC and phosphatidylserine (PS) vesicles; it was suggested that membrane potentials cause an electrostrictive effect associated with increased membrane rigidity. Our results are compatible with this interpretation. However, although membrane potentials modify the diS-C_3-(5) rotational characteristics, the effects are small and are not important in the mechanism of diS-C_3-(5) potential sensitivity.

It has been suggested that one mechanism for the diS-C_3-(5) fluorescence response may be a potential-dependent shift in the location of diS-C_3-(5), resulting in an altered state of aggregation and fluorescence quenching (Ivkova, Pechatnikov, Ivkov & Pletnev, 1983). We tested this hypothesis by examining the dependence of diS-C_3-(5) fluorescence lifetime on membrane potential (Fig. 6 and Table 3). There was no significant effect of a +87 mV potential on lifetime (−2 ± 4 psec), while a −87 mV potential caused a small decrease in lifetime (−9 ±

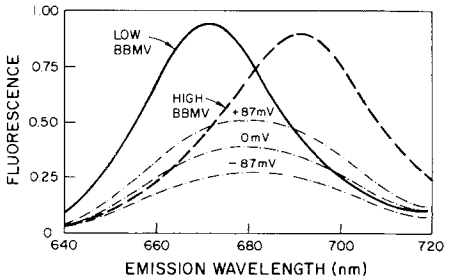

Fig. 7. Effect of membrane potential on diS-C_3-(5) emission spectra. Uncorrected emission spectra (excitation 622 nm, 4 nm slits) for 3 μM diS-C_3-(5) containing BBMV. At 0 mV ($[K^+]_{out}/[K^+]_{in}$ = 150/150 mM) three spectra are shown: 2 μM membrane phospholipid (low BBMV, solid curve), 100 μM membrane phospholipid (0 mV, dashed-dotted curve) and 300 μM membrane phospholipid (high BBMV, dashed curve). For 100 μM membrane phospholipid, +87 and −87 mV potentials were established using $[K^+]_{out}/[K^+]_{in}$ = 150/5 and 5/150 mM. Spectra were recorded within 30 sec after membrane potential was set, at which time dissipation of the KCl gradient did not occur

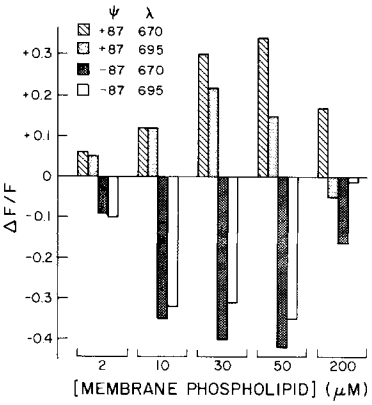

Fig. 8. Concentration dependence of diS-C_3-(5) fluorescence response to membrane potential. +87 and −87 mV membrane potentials were induced with KCl gradients and valinomycin as in Fig. 2 at 3 μM diS-C_3-(5). The dye response measured by fluorescence at 670 and 695 nm (excitation 622 nm), $\Delta F/F$, is the fractional change in fluorescence after valinomycin addition

3 psec). To obtain an order of magnitude estimate of the sensitivity of diS-C_3-(5) lifetime on solvent polarity, assume a linear dependence of lifetime on log dielectric constant. The diS-C_3-(5) lifetime increases by 800 psec for a twofold decrease in solvent dielectric constant (water to ethylene glycol). A 9-psec decrease in lifetime would then correspond to a 0.8% change in dielectric constant. These findings suggest that very little if any change in the diS-C_3-(5) environment occurs with a change in membrane potential.

Model for diS-C_3-(5) Fluorescence Response

The results above indicate that it is the translocation reaction, and not the reorientation/dimerization reaction or the binding reaction, that is driven directly by a membrane potential change. The next set of experiments will show that both the reorientation/dimerization and binding reactions are essential components of the potential-dependent diS-C_3-(5) response mechanism. The quantitative effects of dye/lipid ratio on the fluorescence response and the emission wavelength dependence of the fluorescence response will be used to develop a mathematical model for diS-C_3-(5) fluorescence response to membrane potential.

Figure 7 shows the effects of membrane potential on the diS-C_3-(5) emission spectra. At 0 mV there is a peak at 670 nm at low BBMV which decreases in intensity as BBMV are added because of conversion of aqueous diS-C_3-(5) to nonfluorescent membrane-bound dimer. As more BBMV are added, a new peak at 695 nm is formed which increases in intensity as membrane-bound dimer is converted to membrane-bound monomer. The diS-C_3-(5) fluorescence intensities at 670 and 695 nm are proportional to the concentrations of aqueous diS-C_3-(5) and membrane-bound monomer, respectively. At an intermediate dye/lipid ratio, where all three forms of diS-C_3-(5) are present, a +87-mV potential causes an increase in fluorescence while a −87-mV potential causes a decrease in fluorescence at all wavelengths. If monomer-dimer reequilibration did not occur with a change in membrane potential, the fluorescence intensities at 670 and 695 nm would change in opposite directions since the concentrations of aqueous diS-C_3-(5) and membrane-bound diS-C_3-(5) would be inversely related. Since the intensities change in the same direction, the dimerization reaction is an important component of the diS-C_3-(5) response mechanism.

The quantitative effects of dye/lipid ratio on the diS-C_3-(5) fluorescence response to induced membrane potentials at 670 and 695 nm emission wavelengths are shown in Fig. 8. The magnitude of the response is greatest at [diS-C_3-(5)]/[membrane phospholipid] ratios of 0.06 : 0.1 and becomes very small ($\Delta F/F < 0.02$ at ratios <0.006 and >3 (*not shown*)). The response is generally better at 670 than at 695 nm, and for hyperpolarizing potentials than for depolarizing potentials. It is of note that the responses at 670 and 695 nm are of opposite signs for a +87 mV potential at 200 μM membrane phospholipid.

The experimental observations presented in this and our previous study (Cabrini & Verkman, 1986*a*) have been incorporated into a simple mathe-

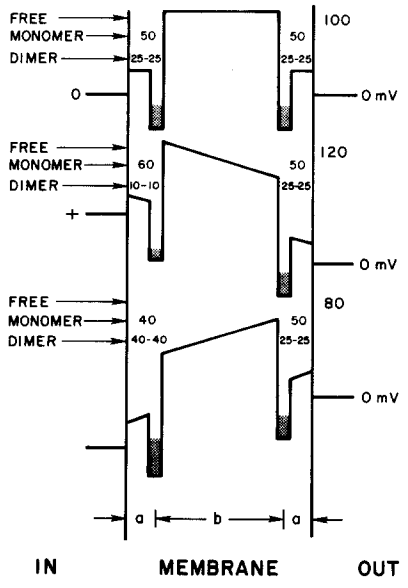

Fig. 9. Potential-sensitive response mechanism for diS-C_3-(5). The postulated profiles for the diS-C_3-(5) binding potential in the absence of membrane potential and in the presence of positive and negative potentials are shown (*see* text). For each condition the hypothetical distributions of 300 diS-C_3-(5) molecules as free dye, and bound monomer and dimer at the outer and inner membrane leaflets are given. *a* and *b* refer to positions for the diS-C_3-(5) binding sites as defined in Eq. (3)

matical model for diS-C_3-(5) potential sensitivity, which is detailed in the Appendix. Some qualitative features of the model are illustrated in Fig. 9. In the absence of a membrane potential (0 mV), the intramembrane potential profile for diS-C_3-(5) binding consists of symmetric minima near the membrane surfaces and a large activation barrier for translocation. The detailed shape of the potential barrier is determined from electrical (monopole, dipole, etc.) and mechanical (steric) interaction characteristics. Total diS-C_3-(5) is distributed among aqueous monomer, and membrane-bound monomers and dimers present at the outer and inner membrane leaflets. The number of intravesicular diS-C_3-(5) molecules is insignificant compared to the number of membrane-bound diS-C_3-(5) molecules.[1] For illustrative purposes it is assumed that a total of 300 diS-C_3-(5) molecules are distributed as 100 aqueous monomers, and 50 membrane-bound monomers and 25 dimers present at each membrane leaflet.

It is assumed that an induced membrane potential results in a composite potential profile containing the 0-mV profile and a linear potential arising from a constant intramembrane electric field. Based on the experimental evidence, it is assumed that the dimerization constant is independent of membrane potential and that membrane potential causes diS-C_3-(5) redistribution between sites at the inner and outer membrane leaflets.

In the presence of an interior positive membrane potential, diS-C_3-(5) is expelled from the membrane, resulting in an increase in the aqueous monomer and in fluorescence at 670 nm. Total diS-C_3-(5) is less at the inner membrane leaflet (80) than at the outer membrane leaflet (100). Because the set point of the monomer-dimer (or in general, monomer-aggregate) equilibrium at each membrane leaflet is determined by the total number of bound diS-C_3-(5) molecules, bound monomer is favored over bound dimer (aggregate) at the inner membrane leaflet. Under these conditions the total number of bound monomers increases from 100 to 110 resulting in an increase in fluorescence at 695 nm. Similarly, an interior negative potential causes diS-C_3-(5) uptake, decrease in fluorescence at 670 nm and increased total diS-C_3-(5) at the inner membrane leaflet. The monomer-dimer equilibrium shifts to favor the dimer (aggregate) so that total bound monomer decreases from 100 to 90, resulting in decreased fluorescence at 695 nm.

The quantitative predictions of the model presented in the Appendix are given in Fig. 10. The model contains a minimal number of assumptions, and the values for all parameters are established from experimental results (*see* Appendix). There is approximate linearity between fluorescence response ($\Delta F/F$) and membrane potential for both hyperpolarizing and depolarizing potentials. In addition, the model predicts greater sensitivity of the fluorescence response for hyperpolarizing membrane potentials than for depolarizing potentials as observed experimentally. The quantitative dependence of $\Delta F/F$ at 670 nm on [membrane phospholipid] is very similar to the experimental results in Fig. 8. $\Delta F/F$ is greatest at intermediate dye/lipid ratios and becomes small at very high or very low dye/lipid ratios.

The detailed dependences of $\Delta F/F$ at 695 nm on [membrane phospholipid] do not fit the experimental results in Fig. 8 closely; however, the general features are correct. At low [membrane phospholipid] the fluorescence response is less at 695 nm than at 670 nm and in the same direction; at high [membrane phospholipid] the sign of $\Delta F/F$ reverses

[1] At equal aqueous and intravesicular diS-C_3-(5) concentrations of 1 μM (0 mV), there would be ~8 diS-C_3-(5) molecules in a BBMV of 0.15 μm radius (1.4×10^{-14} cm^3 volume). The total number of phospholipid molecules per BBMV is ~21,000, assuming an average phospholipid molecular weight of 750 g/mole, density of 0.8 and a 40-Å membrane thickness. At a typical [diS-C_3-(5)] to [membrane phospholipid] ratio of 0.03, there would be ~630 bound diS-C_3-(5) molecules, more than 75 times the number of intravesicular diS-C_3-(5) molecules.

as measured for the positive potential at 200 μM membrane phospholipid (Fig. 8). There are several possible explanations for the inability of the simple model to predict quantitatively accurate $\Delta F/F$ values at 695 nm at high [membrane phospholipid]. The assumption that the only nonfluorescent diS-C_3-(5) species in the membrane are dimers may not be valid. In aqueous solution, West and Pearce (1965) showed that higher order nonfluorescent aggregates are present at high dye concentrations. The presence of an intramembrane monomer-aggregate equilibrium would modify the characteristics of the response curves at 695 nm. In addition, there may be quenching effects of intramembrane monomer or dimer on monomer fluorescence which are neglected in the model. Either of these explanations could account for the inaccuracies of the model at 695 nm; however, we feel that the equilibrium fluorescence titration data are not adequate to mandate inclusion of additional parameters into the model. In addition, there may be inaccuracies in the values of K_d or K_p, or in one of the other assumptions made in the model.

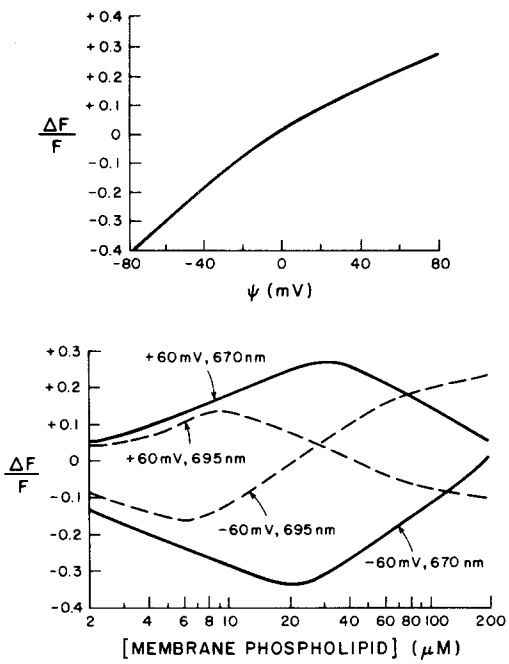

Fig. 10. Mathematical model for diS-C_3-(5) response to membrane potential. Top: $\Delta F/F$ is calculated as a function of ψ for 3 μM diS-C_3-(5), 30 μM membrane phospholipid and 670 nm emission wavelength using Eqs. (A4) and (A7) to (A9), and model parameters given in the Appendix. Bottom: $\Delta F/F$ is calculated as a function of [membrane phospholipid] for 3 μM diS-C_3-(5), $\psi = \pm 60$ mV, and $\lambda = 670$ and 695 nm. The x axis is a logarithmic scale

Discussion

It is important for a number of reasons to define the mechanism of potential sensitivity of fluorescent probes used to measure membrane potential in biological systems. The design of kinetic experiments requires knowledge of the rate at which probe fluorescence responds to perturbations in membrane potential. The optimal excitation and emission wavelengths, and dye and membrane concentrations, must be selected to maximize the fluorescence signal based on an understanding of the dye response mechanism. It is also essential to define non-potential-dependent factors that cause a change in dye fluorescence properties such as solution ionic strength, ionic composition and quenching effects of compounds present in the assay system.

We have focused attention on the mechanism of potential sensitivity of the carbocyanine dye diS-C_3-(5) in biological membranes. The kinetic mechanism and location for diS-C_3-(5) binding was established first in the absence of induced membrane potentials using stopped-flow and phase-modulation fluorescence techniques. The same techniques are now applied to examine how induced potentials modify the binding mechanism. We find that in biological membranes and PC vesicles, induced potentials cause a redistribution of diS-C_3-(5) between sites at the inner and outer membrane leaflets. The redistribution is coupled secondarily to diS-C_3-(5) reorientation/dimerization and solution/membrane partitioning without significant change in the diS-C_3-(5) binding location and rotational characteristics. The diS-C_3-(5) fluorescence response to induced potentials is optimized when fluorescence of the aqueous monomer is monitored (670 nm) and when the dye/lipid ratio is at a mid-equilibrium point (*see* Fig. 8). The time constant for diS-C_3-(5) response to membrane potentials is closely related to the time constant required for the translocation (redistribution) reaction. These findings were incorporated into a mathematical model for diS-C_3-(5) fluorescence response, which is in reasonable agreement with the experimental results.

Many of the individual features of the diS-C_3-(5) response mechanism reported in this paper have been described previously using different experimental approaches. Sims et al. (1974) first studied the response mechanism for a series of cyanines in red cells and PC vesicles. Based on fluorescence and centrifugation binding studies, they showed that partitioning of dye between the aqueous solution and cell or vesicle was dependent on membrane potential. They suggested that dye aggregation occurring within the cell or in the interior regions of the membrane was responsible for the decreased

fluorescence of aqueous diS-C_3-(5). Subsequent studies in the red cell (Hladky & Rink, 1976; Tsien & Hladky, 1978) showed that dye partitioned into the cell interior in response to a hyperpolarizing membrane potential with formation of dimers bound to oxyhemoglobin. These results are consistent with the diS-C_3-(5) response mechanism reported here. When the molar quantity of intravesicular dye is small compared to the quantity of dye bound to the membrane, the dye response mechanism consists of potential-driven translocation with secondary intramembrane monomer-dimer equilibration and membrane-solution partitioning. When large quantities of dye are present in the intracellular compartment because of large cell volume and binding to intracellular contents (red cells), the fluorescence response is enhanced since intravesicular unbound dye is in equilibrium with dye at the inner membrane leaflet. The response rate of the dye to membrane potential changes would decrease because the number of dye units required to cross the intramembrane potential barrier would increase to reach equilibrium at the new membrane potential.

The response of cyanine dyes to changes in membrane potential is enhanced when intracellular or intravesicular aggregation can occur. The effect is most pronounced for interior negative membrane potentials and large cells or vesicles, where high dye concentrations cause aggregation and further inward shift of dye (Loew, Benson, Lazarovici & Rosenberg, 1985). To model intravesicular aggregation, a dye aggregation reaction ($M_f^i \leftrightarrow [M_f^i]_n$) would be added to the mechanism given in Fig. 1. The dye aggregate concentration would then be included in Eq. (A1) and in the subsequent development in the Appendix. Although intravesicular dye aggregation is not important in the vesicle studies described here, it may become very important for measurements in cells and in large vesicles.

Waggoner et al. (1977) studied the time course of absorbance of a series of cyanine dyes in glyceryl-monooleate lipid bilayers in response to a series of square wave voltage pulses. They found a rapid (10 μsec) voltage-induced change in absorbance only when the dye concentrations on each side of the membrane were different. When the dye concentrations were equal, a series of voltage pulses induced a slow (>0.8 sec) increase in the peak absorbance of the dye response pulses; each response pulse had a rise time of ~10 μsec. These results were interpreted on the basis of an on-off mechanism, where membrane potential induces dye partitioning between the membrane and the adjacent aqueous solution. The slow increase in peak absorbance was thought to be related to dye movement across the membrane interior. Our results are in agreement with the potential-driven slow translocation process; however, we do not detect a rapid component for the potential-driven change in diS-C_3-(5) fluorescence (Figs. 4 and 5). Our model would predict a rapid on-off mechanism in addition to the translocation mechanism if the diS-C_3-(5) binding site resided deeper in the membrane than the depth at which the electric field is present (distance a in Fig. 9). Although it is not possible to resolve reaction processes <1 msec with the stopped-flow technique, we found no evidence for any fluorescence change occurring within the instrument dead time based on a comparison between the fluorescence intensity at the beginning of the data trace (Figs. 4 and 5) and the predicted fluorescence intensity at 0 mV. Of course, it is possible that differences between our vesicle preparations and the planar lipid bilayers of Waggoner et al. could explain our inability to identify a very rapid component of dye response. Alternately, if an on-off mechanism is detectable only in the presence of a dye concentration gradient because of diffusion polarization effects at the aqueous interface as suggested above, it would not be possible to study the rapid component using our techniques. Because cell and vesicle studies are performed in the absence of cyanine dye concentration gradients, on-off binding probably does not contribute to the dye response mechanism in these systems.

Ivkova et al. (1983, 1984) have performed a series of equilibrium fluorescence titrations of diS-C_3-(5) in lecithin vesicles and sarcoplasmic reticulum vesicles. They quantitated the amounts of diS-C_3-(5) present in aqueous solution and as membrane-bound monomers and aggregates based on an assumed binding mechanism. They proposed a redistribution mechanism for the diS-C_3-(5) fluorescence response to membrane potential and calculated the theoretical response characteristics of the dye. Our equilibrium titration results and conclusions are in general agreement with those of Ivkova et al. although the modeling approaches differ. In addition, the stopped-flow and phase-modulation results reported here define kinetic features of the diS-C_3-(5) response mechanism, and the distribution and characteristics of the diS-C_3-(5) binding sites which cannot be examined by steady-state fluorescence measurements alone.

We thank Floyd Rector for his support of this project and Nicholas P. Illsley for preparation of placental membranes. This work was supported by N.I.H. grant AM35124, U.C.S.F. grants from the Academic Senate and M.S.C. Clough Fund, and the Hedco Foundation. Dr. Cabrini was supported by Associazione Veneta Fibrosi Cistica and USL 25 Regione Venete of Italy.

References

Barrow, D.A., Lentz, B.R. 1983. The use of isochronal reference standards in phase and modulation fluorescence lifetime measurements. *J. Biochem. Biophys. Meth.* **7:**217–234

Beck, J.C., Sacktor, B. 1978. Membrane potential-sensitive fluorescence changes during Na^+-dependent D-glucose transport in renal brush border membrane vesicles. *J. Biol. Chem.* **253:**7158–7162

Booth, A.G., Kenny, A.J. 1974. A rapid method for the preparation of microvilli from rabbit kidney. *Biochem. J.* **142:**575–581

Booth, A.G., Olaniyan, R.O., Vanderpuye, O.A. 1980. An improved method for the preparation of human placental syncytiotrophoblast microvilli. *Placenta* **1:**327–336

Cabrini, G., Verkman, A.S. 1986*a*. Mechanism of interaction of the cyanine dye diS-C_3-(5) with renal brush-border vesicles. *J. Membrane Biol.* **90:**163–175

Cabrini, G., Verkman, A.S. 1986*b*. Interaction mechanism and localization of potential sensitive cyanine dye binding to brush border membranes. *Biophys. J.* **49:**310*a* (*abstr.*)

Dragsten, P.R., Webb, W.W. 1978. Mechanism of potential sensitivity of the membrane potential sensitive probe merocyanine 540. *Biochemistry* **17:**5228–5240

Gunther, R.D., Schell, R.E., Wright, E.M. 1984. Ion permeability of rabbit intestinal brush border membrane vesicles. *J. Membrane Biol.* **78:**119–127

Hladky, S.B., Rink, T.J. 1976. Potential difference and the distribution of ions across the human red blood cell membrane: A study of the mechanism by which the fluorescent cation diS-C_3-(5) reports membrane potential. *J. Physiol. (London)* **263:**287–305

Huang, C., Thompson, T.E. 1974. Preparation of homogeneous, single-walled phosphatidylcholine vesicles. *Methods Enzymol.* **32:**485–489

Ivkova, M.N., Pechatnikov, V.A., Ivkov, V.G. 1984. Mechanism of fluorescent response of the probe diS-C_3-(5) to transmembrane potential changes in a lecithin vesicle suspension. *Gen. Physiol. Biophys.* **3:**97–117

Ivkova, M.N., Pechatnikov, V.A., Ivkov, V.G., Pletnev, V.V. 1983. Mechanism of fluorescence response of the carbocyanine probe diS-C_3-(5) to change in the transmembrane potential. *Biofizika* **28:**171–184

Kinnally, K.W., Tedeschi, H., Maloff, B.L. 1978. Use of dyes to estimate the electrical potential of the mitochondrial membrane. *Biochemistry* **17:**3419–3428

Lelkes, P.I. 1979. Potential dependent rigidity changes in lipid membrane vesicles. *Biochem. Biophys. Res. Commun.* **90:**656–662

Loew, L.M., Benson, L., Lazarovici, P., Rosenberg, I. 1985. Fluorometric analysis of transferable membrane pores. *Biochemistry* **24:**2102–2104

Sims, P., Waggoner, A., Wang, C., Hoffman, J. 1974. Studies on the mechanism by which cyanine dyes measure membrane potential in red blood cells and phosphatidylcholine vesicles. *Biochemistry* **13:**3315–3323

Steck, T.L., Kant, J.A. 1974. Preparation of impermeable ghosts and inside-out vesicles from human erythrocyte membranes. *In:* Methods of Enzymology. S. Fleischer and L. Packer, editors. Vol. 31, pp. 172–180. Academic, New York

Tsien, R., Hladky, S. 1978. A quantitative resolution of the spectra of a membrane potential indicator, diS-C_3-(5) bound to cell components and to red blood cells. *J. Membrane Biol.* **38:**73–97

Waggoner, A.S. 1976. Optical probes of membrane potential. *J. Membrane Biol.* **27:**317–334

Waggoner, A.S., Wang, C.H., Tolles, R.L. 1977. Mechanism of the potential dependent light absorption changes in lipid bilayer membranes in the presence of cyanine and oxonol dyes. *J. Membrane Biol.* **33:**109–140

West, W., Pearce, A. 1965. The dimeric state of cyanine dyes. *J. Phys. Chem.* **69:**1894–1903

Wright, E.M. 1984. Electrophysiology of plasma membrane vesicles. *Am. J. Physiol.* **246:***F*363–*F*372

Wright, S.H., Krasne, S., Kippen, I., Wright, E.M. 1981. Na^+-dependent transport of tricarboxylic acid cycle intermediates by renal brush border membranes. Effects on fluorescence of a potential-sensitive cyanine dye. *Biochim. Biophys. Acta* **640:**767–788

Received 31 January 1986

Appendix

Model for DiS-C_3-(5) Response Mechanism

A mathematical model is developed to calculate the relative fluorescence response ($\Delta F/F$) to a membrane potential change (ψ) at any dye/lipid ratio and diS-C_3-(5) emission wavelength (λ). Several qualitative features of the model are explained in the text in reference to Fig. 9. Total diS-C_3-(5) (C_t, μM) is present as aqueous monomer (C_o), bound monomer (M_o) and dimer (D_o) at the outer membrane leaflet, and bound monomer (M_i) and dimer (D_i) at the inner membrane leaflet. Conservation of C_t requires

$$[C_t] = [C_o] + [M_o] + 2[D_o] + [M_i] + 2[D_i]. \quad \text{(A1)}$$

Based on the slow, single exponential fluorescence response to membrane potential (Fig. 4) and the lack of effect of potential on the time course of the reorientation/dimerization reaction (Table 1), it is assumed that the intramembrane monomer-dimer equilibrium constant is unperturbed by membrane potential

$$K_d = [M_o]^2/([D_o][L]) = [M_i]^2/([D_i][L]) \quad \text{(A2)}$$

where K_d is a dimensionless dimer dissociation constant and $[L]$ is the membrane concentration expressed as μM phospholipid.

In the absence of a membrane potential (0 mV) it was shown previously that partitioning of diS-C_3-(5) into BBMV can be described empirically using a single-site saturation model

$$[C_o] = [C_t]/(1 + [L]/K_p) \quad \text{(A3)}$$

where K_p is a partitioning constant representing the membrane phospholipid concentration at which the dye is distributed equally between the membrane and aqueous compartments. According to this formulation, parallel partitioning of dye into two membrane compartments (inner and outer membrane leaflets) of equal effective volume (equal $[L]$) but of differing partitioning constants (K_p^1 and K_p^2) would be described by Eq. (A3) with K_p replaced by

$$1/K_p' = 1/K_p^1 + 1/K_p^2 \quad \text{(A4)}$$

where K_p' is an apparent partitioning constant.

According to the model in Fig. 9, an induced membrane potential would alter each K_p in a manner dependent on the magnitude of ψ at the two dye-binding sites

$$K_p^1 = K_p \exp(a\alpha\psi/d)$$
$$K_p^2 = K_p \exp(\alpha\psi[1 - a/d]) \quad \text{(A5)}$$

where a and d are the distances shown in Fig. 9, and α will be taken as an empiric constant which contains the Boltzman constant, temperature and the 'effectiveness' of the membrane potential in inducing dye redistribution. Assuming bound dye monomer and dimer experience similar electrical forces, an approximate relationship for total dye at the inner and outer membrane leaflets is

$$[M_i] + 2[D_i] = ([M_o] + 2[D_o]) \exp(-\alpha\psi[1 - 2a/d]). \quad \text{(A6)}$$

Combining Eqs. (A1) through (A6)

$$[M_o] = \frac{-[L]K_d}{4} + \sqrt{\frac{[L]^2K_d^2}{16} + \frac{[L]^2K_d[C_t]}{2(1 + \exp(-\alpha\psi[1 - 2a/d]))(K_p' + [L])}}. \quad \text{(A7)}$$

The fluorescence at wavelength λ and potential ψ, $F(\lambda,\psi)$ is then given by

$$F(\lambda,\psi) = F_M[M_o](1 + \exp(\alpha\psi[1 - 2a/d])) + F_C[C_t]/(1 + [L]/K_p') \quad \text{(A8)}$$

where F_M and F_C are the fluorescence intensities (intensity units/μM diS-C_3-(5)) of bound and aqueous monomer, respectively. The fluorescence response of the dye ($\Delta F/F$) is then given by

$$\Delta F/F = [F(\lambda,\psi) - F(\lambda,0)]/F(\lambda,0). \quad \text{(A9)}$$

Equations (A4) and (A7) through (A9) provide a simple model for the response of diS-C_3-(5) fluorescence as a function of $[C_t]$, $[L]$ and ψ. The physical parameters describing the system: $a\alpha/d$, α K_p, K_d, $F_M(\lambda)/F_C(\lambda)$ are required to calculated $\Delta F/F$ values.

For the model predictions shown in Fig. 10, the parameters were estimated as follows. $F_M(670)/F_C(670) = 0.3$ and $F_M(695)/F_C(695) = 3.0$ are estimated from fluorescence emission spectra of 3 μM diS-C_3-(5) in the presence of 0 and 400 μM membrane phospholipid (Fig. 1 of Cabrini & Verkman, 1986*a*). The parameter $\frac{a\alpha}{d}$ is set equal to zero based on the lack of any rapid component to the fluorescence response, and $\alpha = 0.017$ is chosen to match the measured $\Delta F/F$ at +87 mV, 670 nm. $K_p = 17$ μM and $K_d = 0.0013$ are taken from the fluorescence titrations at 0 mV described previously (Fig. 2 of Cabrini & Verkman, 1986*a*).